Vol. 48 No. 1 Journal of the Communications Research Laboratory March 2001
Printed in Tokyo, Japan pp. 151–158

4.5 Evaluation of GPS-based Ionospheric TEC Estimation and Application to Pulsar VLBI Observation

By
Mamoru SEKIDO, Tetsuro KONDO, Eiji KAWAI, Yuko HANADO,
and Michito IMAE

ABSTRACT

We evaluated the accuracy of GPS-based TEC measurements by comparing the results with S/X dual frequency VLBI experimental data. The Global Ionosphere Maps (GIMs) generated by CODE (Center for Orbit Determination in Europe) is one of the most accurate and freely available GPS-derived ionosphere maps, so we evaluated the accuracy of the GIM/CODE maps. Sekido et al. have demonstrated that ionospheric group delays computed from GIM/CODE agree with the ionospheric TEC measured by VLBI to an accuracy of 3-10% of the total contribution of TEC to the VLBI observation. Following on this research, this paper presents a comparison between the phase delay rate calculated from the GIM/CODE and phase delay rate measured by VLBI observations. The correlation between the ionospheric phase delay rates obtained from VLBI observation and those obtained from the GIM/CODE data were not as high as in the case of group delay. The main reason for the lower coincidence is that the GIM/CODE data does not contain short period variation components in the temporal and spatial domains. Using the GIM/CODE data, we have applied ionospheric delay correction to single-band astrometric VLBI data. This resulted in improved consistency between the group delay and observed phase delay rate, and estimated pulsar coordinate solutions that were more stable than those obtained without ionosphere correction. The proper motion obtained from this ionospheric-delay-corrected VLBI data agrees well with the other proper motion measurements.

Keywords: GPS, Ionospheric total electron content (TEC), VLBI, Pulsar

1. Introduction

When VLBI is used to observe the positions of celestial radio source, the observations are usually made at a single frequency except when observing with a geodetic VLBI antenna equipped with an S/X band receiver system. For example, the radio flux density from pulsars[1] decreases sharply in inverse proportion to roughly the second or third power of frequency, so frequencies in the 2 GHz or below are used when making VLBI observations. In such observations, since the observation frequency is relatively low and in single frequency band, the largest error source to observation is the delays by the ionosphere. As an approach to compensate for the ionospheric delay in astrometric VLBI observations, GPS-based ionosphere measurements have been examined[17]-[18].

GPS satellites broadcast signals at two frequencies: L1 (1575.42 MHz) and L2 (1227.60 MHz). It is possible to measure the ionosphere electron content by using the dispersive properties of the ionospheric delay. Regional ionosphere inferred from GPS observation or global ionospheric model developed by the CODE (GIM/CODE) were compared with ionospheric delay obtained by dual frequency VLBI observations. And it was demonstrated that ionospheric effect in VLBI observation can be compensated in 3-10% accuracy by using the GIM/CODE global ionosphere map[3]. On the other hand, the amount of phase delay and the phase delay rates are also important observables not only for VLBI but also for the precise space measurement techniques such as space crafts navigation[4] and planetary ionosphere research. Although the International Reference Ionosphere (IRI)[5]—a standard ionospheric model—is also improving, it is not accurate enough to meet the requirements of precise measurements such as those mentioned above. Following the evaluation research of group delay accuracy of the GIM/CODE[3], phase delay rates were computed from the GIM/CODE, and they are compared with the results of VLBI observations. We also discuss the results of applying the GIM/CODE ionospheric correction to the pulsar VLBI observations data obtained at 1.4 GHz and 2.2 GHz during from 1995 to 1998.

2. Radio Wave Propagation in Ionospheric Plasma

Although individual particles in an ionized gas move randomly, Cold Plasma theory—which describes the average group motion of charged particles—can be used to describe the interaction between electromagnetic waves and a plasma when electromagnetic waves pass through it[6]. Since ions are about one thousand times heavier than electrons, the electrons mainly interact with microwave. The equation of motion of electron, which describes averaged group motion of electrons, is given by the following formula, where v_d is the electron drift velocity, B is the geomagnetic field flux density of the Earth, and ν is an electron's average scattering probability per unit time.

$$m\frac{dv_d}{dt} = -e(E+v_d\times B)-mv_d\nu \quad \cdots\cdots(1)$$

Here, e and m are the charge and mass of an electron,

respectively. Although the magnetic field of an electromagnetic wave also affects on the motion of electrons by a Lorenz force, its magnitude is only of the order of $v_d \times \mu_0 H = n|v_d||E|/c$ (n =refractive index; c = speed of light), even when the electron is moving perpendicular to the magnetic field. This is smaller than the electric field by a factor of $n|v_d|/c$, so is usually ignored. From this equation of motion and Maxwell's formula, the Appleto n-Hartree's formula is derived:

$$n^2 = 1 - \frac{2X}{2(1-jZ) - \frac{Y^2\sin^2\theta}{1-X-jZ} \pm \sqrt{\frac{Y^4\sin^4\theta}{(1-X-jZ)^2} + 4Y^2\cos\theta}} \quad \cdots\cdots (2)$$

where θ is the angle between the magnetic flux B and the wave vector k which indicates the direction in which the radio wave propagates, $X = \omega_p^2/\omega^2$, $Y = \Omega_e/\omega$, $Z = \nu/\omega$, and $\omega_p = \sqrt{N_e^2/\varepsilon_0 m}$ is the plasma angular frequency, $\Omega_e = eB/m$ is the cyclotron (Larmor) angular frequency, $\omega = 2\pi f$ is the observation radio angular frequency, N_e is the electron density, and $j = \sqrt{-1}$. When the observation frequency is sufficiently larger than the plasma frequency, cyclotron frequency and electrons collision frequency ($X \ll 1$, $Y \ll 1$, $Z \ll 1$), Equation (2) can be approximated as follows:

$$n \approx \sqrt{1 - \frac{X}{1-jZ \pm Y\cos\theta}} \approx 1 - \frac{1}{2}X(1 + jZ \mp Y\cos\theta) \quad \cdots (3)$$

where the plus and minus symbols correspond to right hand circular polarization (RHCP) and left hand circular polarization (LHCP), respectively (It should be noted that the definitions of polarization is the opposite to that used in radio astronomy). As can be seen from Equation (3), the refractive index varies with radio frequency, and thus a medium of this sort is referred to as a dispersive medium. The speed v_g (group velocity) of signals in a dispersive medium differs from the phase velocity v_p. If third-order and higher terms in X, Y and Z are ignored, these velocities can be approximated by the following formulae:

$$v_p = \omega/k = c/n \approx c\left\{1 + \frac{X}{2}(1 - jZ \mp Y\cos\theta)\right\} \quad \cdots\cdots (4\text{-a})$$

$$v_g = d\omega/dk = \frac{c}{n + \omega dn/d\omega}$$

$$\approx c\left\{1 - \frac{X}{2}(1 + X + jZ \mp 2Y\cos\theta)\right\} \quad \cdots\cdots (4\text{-b})$$

Furthermore, if terms in X^2 can also be ignored, the excess delay compared with the propagation through a vacuum is expressed as follows:

$$\Delta\tau_p = -\frac{C_X}{\omega^2}\left\{(1 + jZ)\int ndl \mp \frac{C_Y}{\omega}\int nB\cos\theta dl\right\} \quad \cdots\cdots (5\text{-a})$$

$$\Delta\tau_g = +\frac{C_X}{\omega^2}\left\{(1 + jZ)\int ndl \mp \frac{2C_Y}{\omega}\int nB\cos\theta dl\right\} \quad \cdots\cdots (5\text{-b})$$

where $C_X = e^2/2m\varepsilon_0 c$, and $C_Y = e/m$ The collision rate of electrons reaches a maximum of about 10^3 sec^{-1} at altitudes of 200-400 km where the electron density is the highest, so $Z \leq 10^{-7}$ at an observation frequency of 1.4-2 GHz, and the cyclotron frequency due to the geomagnetic field is around 1 MHz, so $Y \leq 10^{-4}$, thus terms of Y and Z are also ignored here. To measure the TEC with an accuracy of 0.01% (0.01 TECU), it may be necessary to consider the effects of the geomagnetism. And when this sort of high precision is required, it may also be necessary to consider the propagation path bending effect due to refraction in the ionosphere. According to the results of numerical simulations using ray tracing technique, excess path length of several cm in the 1.5 GHz band can be caused by the ray path bending at low elevation angle during extreme ionospheric state[7].

3. The CODE Global Ionospheric Model

The Center for Orbit Determination in Europe (CODE), which is one of the analysis centers of the International GPS Service (IGS), has been established at Bern University in Switzerland. And it is continuously generating precise ephemeredes of GPS satellites by using the GPS observation data of the IGS network. The same IGS observation data is also being used to estimate global ionospheric electron distribution data (Global Ionosphere Map: GIM) and this data is being published on the internet[8]-[10] (http://www.aiub.unibe.ch/ionosphere.html). The method used to estimate the CODE ionospheric map is outlined below.

Let ρ_i^k is the geometric distance between a satellite k and a receiver i, and the GSP carrier phase is an observable, then the pseudo distance between the satellite and the earth is expressed as follows:

$$L_{i,1}^k = \rho_i^k + c(\Delta t_i - \Delta t^k) + \Delta\rho_{i,trop}^k - I_i^k + \lambda_1 B_{i,1}^k + \varepsilon_1 \quad \cdots\cdots (6\text{-a})$$

$$L_{i,2}^k = \rho_i^k + c(\Delta t_i - \Delta t^k) + \Delta\rho_{i,trop}^k - \xi_1 I_i^k + \lambda_2 B_{i,2}^k + \varepsilon_2 \quad \cdots\cdots (6\text{-b})$$

where λ is the wavelength at which the pseudo range is measured. B_i^k is the phase uncertainty, but since λB_i^k includes not only an integer bias (N_i^k) as $\lambda(N_i^k + \delta N_i^k) + c(b^k - b_i)$ but also hardware bias comprising a phase jump (δN_i^k), the receiver (b_i) and the satellite (b^k) hardware offset, B_i^k is generally a real number instead of an integer. I_i^k is the excess path length by the ionosphere measured with wavelength of L_1. $\Delta\rho_{i,trop}^k$ is the delay caused by the troposphere, Δt_i is clock offset of receiver i. Δt^k is the clock offset of satellite k. ε is the random error, and $\xi_1 = \nu_1^2/\nu_2^2$ where ν_1 and ν_2 are the observation frequencies of L_1 and L_2 respectively.

For the sake of simplicity, random errors are disregarded in the following discussion. The difference of carrier phases between L_1 and L_2 (Zero Difference) by using Equation (6) leads to an expression (Geometry-Free Linear Combination) that does not depend on the clock offset nor the geometrical relation.

$$L_3 = L_{i,1}^k - L_{i,2}^k = \xi_2 I_i^k + B_{i,3}^k \quad \cdots\cdots (7)$$

where $\xi_2 = 1 - \xi_1 = 1 - \nu_1^2/\nu_2^2$ and $B_{i,3}^k = \lambda_1 B_{i,1}^k - \lambda_2 B_{i,2}^k$. If we take double phase difference of L_3 between the satellites and between the receivers, the new linear combination is expressed by the ionospheric TEC in the zenith direction (VTEC) and the mapping function F(e1) as follows:

$$L^{kl}_{i,j,3}=(L^{k}_{i,3}-L^{k}_{j,3})-(L^{l}_{i,3}-L^{l}_{j,3})=\xi_2\xi_3(F(el)\,VTEC)^{kl}_{ij}+B^{kl}_{i,j,3} \quad \cdots\cdots(8)$$

where $\xi_3(\text{constant}) = C_X c = 0.1623\ (meter/TECU))$, $F(el)$ is an ionosphere mapping function defined as the ratio of the TEC in the line of sight at an elevation angle of el to the TEC in the zenith direction, and $B^{k}_{i,j,3}=\lambda_1 N^{kl}_{i,j,1}-\lambda_2 N^{kl}_{i,j,2}$. For the mapping function we assumed a single-layer spherical shell model and used an constant ionosphere height of H=450 km :

$$F(El,\ H)=\frac{1}{\cos\left\{\sin^{-1}\left[\frac{R}{R+H}\cos(El)\right]\right\}} \quad \cdots\cdots(9)$$

Since double phase difference is obtained in this way, the bias originating in the receiver and the satellite hardware is canceled, so the phase uncertainty takes on an integer value. Furthermore, if integer bias $N^{kl}_{i,j,1}$ and $N^{kl}_{i,j,2}$ can be established, $B^{k}_{i,j,3}$ becomes known. At CODE, the GPS data for at least 140 IGS observation points throughout the world are used to solve the phase uncertainty by geometric analysis using the double phase difference. By using Equation (8) as the observation equation and using 12th-degree eighth-order (149 parameter) spherical harmonic functions as ionosphere model, global ionosphere maps have been estimated by the least squares method[8][9].

When the delay of P codes is used as the observable, uncertainly of the hardware code bias becomes a problem[3][11]. But in the CODE's analysis, the phase delay is an observable and the analysis is performed by double

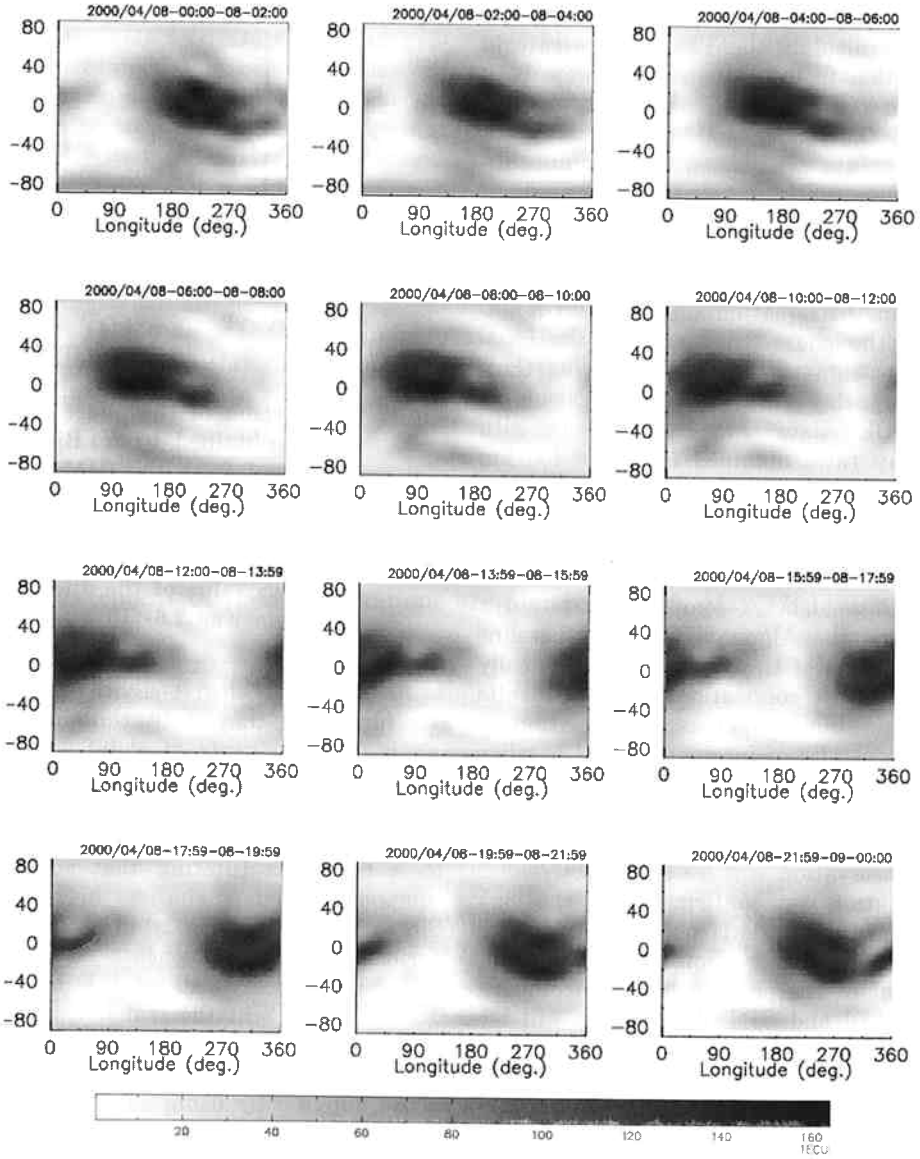

Fig. 1 Global ionospheric electron density distribution at two-hour intervals on April 8, 2000 (UT) estimated by the CODE. This figure shows the ionospheric maps at two-hour intervals, starting from the top left. The horizontal axis is the geographical longitude, and the vertical axis is the geographical latitude.

phase difference, so such problems do not arise. Since 1995, the CODE has continuously published daily ionospheric maps in the IONEX format[9] and Bernese ION File format, and related subroutines on the internet*. An example of the CODE ionosphere map (GIM) is shown in Fig. 1. This map was produced from the Bernese ION file for April 8, 2000. Since geomagnetic pole has offset from geographical pole, the regions of high electron density—which vary along the geomagnetic equator—form a roughly sinusoidal pattern.

4. Comparison of the Phase Delay Rate Between the GIM/CODE and VLBI Observations

A comparison of ionospheric delay between the GIM/CODE and VLBI observation data is described in a separate study[3]. Here we will concentrate on the accuracy evaluation of phase delay rate calculated from the GIM/CODE data. To calculate the TEC change rate in the line of sight direction from an ionosphere map, both the change in elevation angle of the line of sight and the temporal variation of the ionosphere have to be taken into account. Here, 5 points were taken at 10 minute intervals over the period spanning 20 minutes either side of the target time epoch. The elevation angle and TEC in the line of sight were calculated at 5 points, and the TEC change rate in the line of sight direction was obtained by numerical derivation. As Equation (5) shows, it is important to note that the phase delay rate of the ionosphere has the opposite sign to the group delay of that. The ionospheric phase delay rate which was calculated from the GIM/CODE data was compared with ionospheric phase delay rates obtained from the 100 km baseline VLBI data (Key Stone Project: KSP)[12], and with ionospheric phase delay rates obtained from intercontinental geodetic VLBI observations conducted by the International VLBI Service (IVS)[13].

As an example, Fig. 2 shows comparative data for the phase delay rate on the Algonquin-Wettzell baseline on July 18, 2000. As results of these comparison basically there was hardly any visible correlation with the results of short baseline observations, whereas a correlation of about 0.6 to 0.8 as the results of intercontinental baseline observations was eventually confirmed. The average correlation coefficient was about 0.6 and the rms residual was 3×10^{-3} TECU/sec, whereas the error of the phase delay rate of VLBI observation was 5×10^{-4} TECU/sec.

Although a correlation was confirmed with the long base line data, it is clear that this is not a level of accuracy that can be required for correction. Possible reasons for the less agreement of the phase delay rate comparison results between VLBI and GPS observations will be:

(i) The phase delay rate is derived from the numerically derivation of TEC calculated from GIM/CODE maps. However, the GIM/CODE consists of two-hour interval TEC maps, so they do not include short-term temporal variations of TEC.

(ii) Since the GIM/CODE ionosphere maps are derived using a 12th-degree-eighth order spherical harmonic functions, they only contain the minimum spatial scale components of about 2500 km in the longitude direction and 1700 km in the latitude direction.

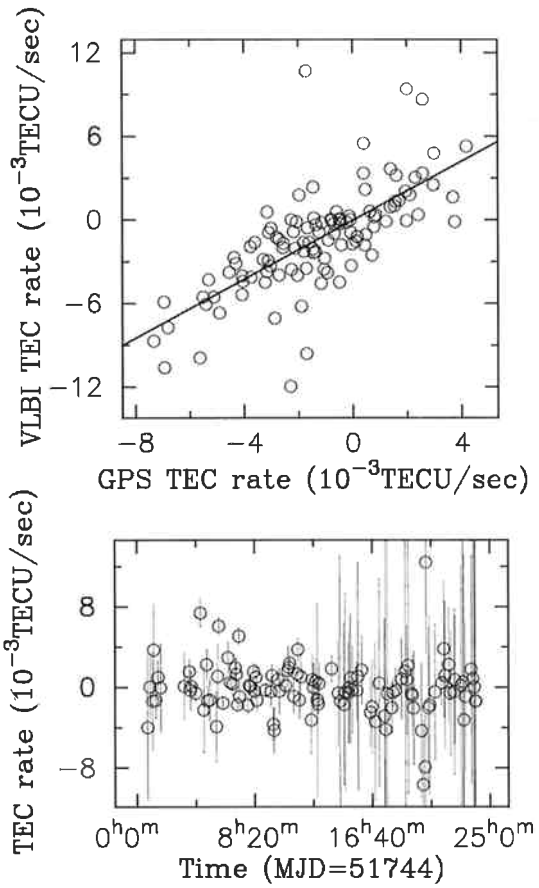

Fig. 2 Comparison of the phase delay rate of the ionosphere obtained by VLBI observations and that calculated from the GIM/CODE data. The VLBI data for the Algonquin-Wettzell base line on July 18, 2000 was acquired from the IVS data archive. The correlation coefficient was 0.7, and the RMS value of the difference between the two data sets was 2.6×10^{-3} TECU/sec.

From a signal processing viewpoint, the derivative operation used to obtain the phase delay rate corresponds to a high-pass filtering that suppresses low frequency components and emphasizes high frequency components. Since the GIM/CODE data, which does not include short period variation components in both time and space domain, phase delay rate of the derived from GIM/CODE does not represent the real ionosphere variation.

Saito et al. have detected electron density waves in the ionosphere with high spatial frequencies in the skies above Japan[15] by using data from the Geographical Survey Institute's GPS observation network (GEONET)[14]. Unless an ionosphere map can be made which contains the short period variation components of ionosphere TEC

*http://www.aiub.unibe.ch/ionosphere.html

with high temporal and spatial resolution, it will probably be of no use for correcting the phase delay rate of VLBI or correcting the range rate of interplanetary probes. Alternatively, it will be possible to use the GEONET data to construct an ionospheric model above Japan, which may be capable of contributing to the abovementioned space measurement techniques.

5. Application of Ionospheric Delay Correction to Pulsar VLBI Observations

In 1995, CRL and the Lebedev Physical Institute in Russia began a series of VLBI pulsar observations. These involved making astrometric VLBI observations of the pulsar PSR0329+54 at 1.4 GHz in March 1995 and May 1996, and at 2.2 GHz in May 1998. Since pulsars have the property whereby their radio intensity drops rapidly in inverse proportion to the second or third power of their frequency, they cannot be used to measure the ionosphere by simultaneous observations at 2 GHz/8 GHz as in geodetic VLBI observations. Since the ionospheric delay increases in inverse proportion to the square of frequency, it constitutes the largest error source in single-frequency VLBI observations at 1.4 GHz and 2 GHz.

We therefore tried to correct for ionospheric delay in the VLBI observations by using the GIM/CODE. It is expected that the GIM/CODE data can be used to compensate for the ionospheric delay in VLBI observations with an error of 3-10% of the TEC affecting the observations[3], in other words it should be possible to eliminate at least 90% of the ionospheric delay. As mentioned above, the GIM/CODE data is not very effective at correcting the phase delay rate, but since any additional errors introduced by this correction should only be slight, we compensated both the group delay and the rate of change of phase delay.

To estimate the pulsar's position, we used the CALC8.2/SOLVE5.25 software package, which was for VLBI geodetic/astrometric analysis. And ICRF sources, whose coordinates are well known, are used to calibrate the VLBI parameters such as the clocks and atmospheric parameters. Table 1 lists the pulsar positions obtained from least square (LSQ) estimations in several cases of analysis conditions. Since group delay and phase delay sign is opposite, phase delay rate and group delay is expected to make some conflict in the LSQ estimation when ionospheric delay is not appropriately compensated. Thus two cases of observable (group delay plus phase delay rate and group delay only) and ionospheric delay correction on and off, totally four cases of analysis were examined. In Fig. 3, the estimated source coordinates are plotted separately for right ascension and declination. The arrow in these figures show the proper motion of PSR0329+54 measured by Harrison et al.[16] using the MARLIN interferometer (UK) as a reference.

When ionospheric correction is performed, formal errors were reduced and reliable pulsar's coordinates in the ICRF were obtained. Proper motion of the pulsar were derived from the series of pulsar coordinates and it coincide within one sigma level with Harrison et al.[16]'s result. Table 2 lists the the proper motion estimated from the results of observations and analysis at three epochs.

Table 1 The estimated positions of pulsar PSR0329+54 in the ICRF. These positions were obtained by least-square analysis with the only group delay as the observable (D), with the group delay and phase delay rate as the observable (D&R), and with/without ionospheric correction using the GIM/CODE data. The epochs of these observations are March 14, 1995, May 12, 1996, and May 25, 1998.

Epoch	ION Corr.	Observable	R.A.	σ_α(sec.)	Dec.	σ_δ(arc sec)
1995.20	×	D	59.376	0.0009	43.511	0.008
	×	D&R	59.375	0.003	43.510	0.02
	○	D	59.376	0.0008	43.506	0.006
	○	D&R	59.376	0.0009	43.507	0.006
1996.36	×	D	59.379	0.002	43.509	0.01
	×	D&R	59.379	0.002	43.491	0.01
	○	D	59.379	0.001	43.489	0.008
	○	D&R	59.379	0.001	43.485	0.008
1998.40	×	D	59.383	0.0005	43.477	0.004
	×	D&R	59.384	0.0006	43.478	0.004
	○	D	59.383	0.0008	43.465	0.006
	○	D&R	59.383	0.0008	43.465	0.005

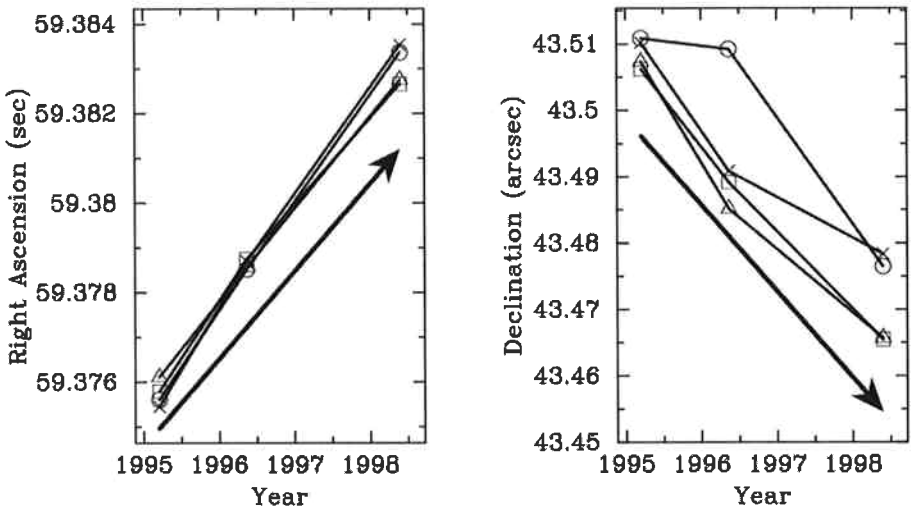

Fig. 3 The position and proper motion of PSR0329+54 in the ICRF. This figure shows the results of VLBI observations made between Japan and Russia at three epochs 1995.20, 1996.36 and 1998.40 under the following analysis conditions: ○ = without ionospheric delay correction, only group delay as observable; × = without ionospheric delay correction, group delay and phase delay rate as observable; △ = with ionospheric delay correction using the GIM/CODE data, only group delay as observable; □ = with ionospheric delay correction using the GIM/CODE data, group delay and phase delay rate as the observable. The arrow shows the proper motion measured by Harrison et al as a reference. When ionospheric correction is performed, the results are more stable and closely coincide with the results of Harrison et al.

Table 2 The proper motion and source coordinates of pulsar PSR0329+54 at 1996.0 on the ICRF obtained by least squares. The right ascension of the coordinate values represents the offset in arc seconds from 3^h32^m, and the declination represents the offset in arc seconds from 54°34'. This table shows the results obtained with and without GIM/CODE ionospheric correction when using only the group delay as observable (D), and when using group delay and the phase delay rate as the observable (D&R). The proper motion of PSR0329+54 measured by Harrison et al. is written in the bottom row for comparison.

Ion Corr.	Observable	$\mu_\alpha(mas/yr)$	$\mu_\delta(mas/yr)$	R.A. (sec.)	Dec. (arc sec)
×	D	21.6±6	−8.4±4	59.378 ±0.0016	43.498±0.009
×	D&R	21.1±3	−11.7±2.6	59.3776±0.0006	43.505±0.005
○	D	18.1±3	−12.7±2.4	59.3777±0.0006	43.495±0.004
○	D&R	18.6±3	−12.6±2.5	59.3776±0.0006	43.595±0.004
Harrison et al		17±1	−13±1	−	−

6. Conclusion

6.1 Comparison of GPS ionospheric maps with VLBI observations

We have calculated the phase delay rate by numerical derivation from the global ionospheric maps (GIM/CODE) which were generated by the Bern University by using IGS GPS observation network. By comparing the phase delay rate derived from GIM/CODE with the results of VLBI measurements, we have made clear that although a correlation coefficient of around 0.6 to 0.8 is achieved on intercontinental baselines, this technique is insufficient for the correction of VLBI observation data.

The GIM/CODE data is modeled with a temporal resolution of two hours and a spatial resolution of about 2500 km in the longitude direction and about 1700 km in the latitude direction. It seems that the absence of components with shorter temporal/spatial periods, which affect the calculation of the phase delay rate, is a major reason why precise results were not obtained for the phase delay rate.

Although the GIM/CODE maps were found to be insufficient for compensating the phase delay rate due to constraints on the observation system, it should be possible to use data from GEONET—which comprises almost a thousand GPS observation points over the whole of Japan—to draw up a TEC map of the local electron distribution above Japan with extremely high temporal and spatial resolution. If this can be put into practice, then it should provide an effective means for correcting VLBI

data obtained on baselines within Japan, and for correcting the range and range rate of deep space craft tracking stations in Japan.

6.2 Using the GIM/CODE data to correct VLBI pulsar observations

The GIM/CODE ionospheric maps are effective for correcting the group delay caused by the ionosphere[3]. We used the GIM/CODE data to correct for ionospheric delay in the astrometric VLBI data for pulsar observations made in March 1995, May 1996 and May 1998 between the Kashima 34 m antenna and a 64 m antenna in Russia (over a 7,000 km baseline), and compared these results with the results obtained without correction. Then we found that the corrected results resolved the inconsistencies between the observed group delay and the phase delay rate, providing a more stable solution. The corrected results were also more consistent with the results of the pulsar's proper motion measurements by others.

We have thus verified that estimating the amount of ionospheric delay from ionospheric maps drawn up from GPS observations (GIM/CODE) is an effective means for correcting single-frequency VLBI observations.

Acknowledgments

We would like to thank Stefan Schaer of Bern University in Switzerland for providing the global ionospheric TEC map data. We would also like to thank everyone in the Keystone Project team and everyone in the radio astronomy applications group for their support on this research. IVS archive data was used as a source of intercontinental baseline VLBI data. The research regarding GPS-based ionospheric delay correction was supported by the CRL support foundation. The VLBI pulsar observations on the Japan-Russia baseline were made as part of a collaborative study between CRL and the Lebedev Institute of Physics in Russia. For their valuable assistance in this project, we would like to thank Y.P. Ilyasov, V.V. Oreshko and A.E. Rodin of the Lebedev Institute of Physics, and B.A. Poperechenko of the Moscow Power Engineering Institute.

References

(1) Shibazaki, N., "Neutron stars and pulsars", *Baifukan*, 1993.

(2) Sekido, M, Imae, M., Hanado, Y., Ilyasov, Y. P., Oreshko, V. V., Rodin, A. E., Hama, S., Nakajima, J., Kawai, E., Koyama, Y., Kondo, T., Kurihara, N., and Hosokawa, M., "Astrometric VLBI Observation of PSR0329+54", PASJ, 51, pp.595-601, 1999.

(3) Sekido, M., Kondo, T., Kawai, E., and Imae, M., "Precise evaluation of ionospheric delay by GPS", Technical report of the IEICE SANE2000-142, pp.61-68, 2001.

(4) Heki, K., Matsumoto, K., and Folberghagen, R., "Three-dimentional tracking of a lunar satellite with differential very-long-baseline-interferometry", Advances in Space Research Vol.23, 11 pp.1821-1824, 1999.

(5) "International Reference Ionosphere-Past, Present, Future", Adv. Space Res., 13, No.3, pp.3-23, 1993.

(6) Maeda, K., Kimura, I., "Modern electromagnetic wave motion theory", *Ohmsha*, 1984.

(7) Brunner, F. K., and Gu, M., "An Improved Model for Dual Frequency Ionospheric Correction of GPS observations", Manuscripta Geodetica, 16, 205-214, 1991.

(8) Schaer, S., Beutler, G., and Rothacher, M., "MAPPING AND PREDICTING THE IONOSPHERE", Proc.IGS Analysis Center Workshop 1998, ESA/ESOC Darmstadt in Germany, February 9-11 1998, pp.307-318, 1998.

(9) Schaer, S., "Mapping and Predicting the Earth's Ionosphere Using the Global Positioning System", Ph.D.thesis at Bern University, 1999.

(10) Schaer, S., Gurtner, W., and Feltens, J. "IONEX: The ionosphere Map EXchange Format Version 1", Proc. of IGS Analysis Center Workshop, ESA/ESOC Darmstadt in Germany, February 9-11 1998, pp.233-247, 1998.

(11) Sardón E., Ruis, A., and Zarraoa, N., "Estimation of the transmitter and receiver differential biases and the ionospheric total electron content from Global Positioning System observations", Radio Sci. 29, pp.577-586, 1994.

(12) Yoshino, T., "Overview of the Key Stone Project", Journal of the Communications Research Laboratory, 46, pp.3-6, 1999.

(13) IVS Archive data, http://ivscc.gsfc.nasa.gov/service/products.html, 2000.

(14) Miyazaki, S., Saito, T., Sasaki, M., Tanaka, Y., and Masaharu, H., "Expansion of GSI's nationwide GPS array", Bull. Geogr. Surv. Inst. 43. pp.23-34, 1997.

(15) Saito, A., and Fukao, S., "High resolution mapping of TEC perturbations with the GSI GPS network over Japan", Geophys. Res. Lett., 25, pp.3079-3082, 1998.

(16) Harrison, P. A., Lyne, A. G., and Anderson, B., "New determination of the proper motion of 44 puls ars", Mon. Not. R. Astron. Soc., 261, pp.113-124, 1993.

(17) Ros, E., Marcaide, J. M., Guirado, J., C., Sardón, E., and Shapiro, I. I., "A GPS-based method to model the plasma effects in VLBI observations", Aston. Astrophys, 256, pp.357-362, 2000.

(18) Pérez-Torres, M. A., Marcaide J. M., Guirado, J. C., Ros, E., Shapiro, I. I., Ratner, M. I., and Sardón, "Towrds global phase-delay VLBI astrometry: observations of QSO 1150+812 and BL 1803+784", Astron. Astrophys., 360, pp.161-170, 2000.